PERGAMON

International Journal of Solids and Structures 37 (2000) 5813–5827

INTERNATIONAL JOURNAL OF SOLIDS and STRUCTURES

www.elsevier.com/locate/ijsolstr

Axisymmetric vibration analysis of rotating annular plates by a 3D finite element

Chorng-Fuh Liu*, Ju-Feng Lee, Ying-Te Lee

Department of Mechanical Engineering, National Sun Yat-Sen University, Kaohsiung 80424, Taiwan

Received 2 July 1998; in revised form 8 June 1999

Abstract

The axisymmetric vibration of spinning isotropic annular plates is herein analyzed by a modified axisymmetric finite element. Due to the three-dimensional-elasticity nature of the present approach, all the initial stresses induced by the centrifugal force are calculated and taken into account in the augmented strain energy expression, while only two are considered in the conventional analyses. Also, the whole three velocity components are considered in the inertial term instead of only one by conventional approaches. Natural frequencies of annular plates with different ratios of inner-to-outer radius, ratios of thickness-to-radius, rotational speeds, and boundary conditions are derived by the present approach and are compared with those by a plate-theory approach. © 2000 Elsevier Science Ltd. All rights reserved.

Keywords: Axisymmetric vibration; Annular plate; Finite element

1. Introduction

The vibration of rotating annular disks has been studied by a number of investigators, for e.g., Barasch and Chen (1972), Eversman and Dodson (1969), Kirkhope and Wilson (1976), Lee and Ng (1995), Nigh and Olson (1981), Rajguru and Sundararajan (1982), Sinha (1987) and Wilson and Kirkhope (1976). More information can also be found in Leissa (1977, 1981, 1987). All of these researches are based on plate theories, either classical plate theory or the Mindlin plate theory, and the rotating effect is taken into account through only the in-plane stresses σ_r and σ_θ induced by the rotation of the annular plate. Also, only the inertial term of transverse motion of plates is considered. Because of the two-dimensional-elasticity nature of plate theories, the behaviors through the thickness of the plates

* Corresponding author. Fax: +886-7-525-4299.
E-mail address: liucf@mail.nsysu.edu.tw (C.-F. Liu).

0020-7683/00/$ - see front matter © 2000 Elsevier Science Ltd. All rights reserved.
PII: S0020-7683(99)00256-5

are not easy to reveal and some boundary conditions are just impossible to specify or to impose. To circumvent the disadvantages of the plate theories, Liu and Chen (1995) employed an axisymmetric finite element to analyze the axisymmetric vibration of circular and annular plates, wherein the accuracy and validation of the approach are justified and some results not otherwise available in the literature are shown.

In the present study, the approach by Liu and Chen (1995) is extended to include the rotational effects. Due to the three-dimensional-elasticity nature of the method, all rotation-induced stresses are calculated first and are considered later in the vibration analyses (compared to only two stresses, σ_r and σ_θ, in the conventional analyses) and all velocity components in the r, θ, z directions are included in the kinetic energy term, instead of only the conventional $\partial w/\partial t$ in the transverse direction. Vibrations of rotating annular plates with different ratios of inner-to-outer radius, ratios of thickness-to-radius, rotating speeds and boundary conditions are analyzed, and the results are compared to those obtained by a plate-theory-based approach.

2. Formulation

To analyze the axisymmetric vibration of rotating annular plates, a modified axisymmetric finite element is employed with the displacement field as

$$u = u(r, z, t)$$

$$v = v(r, z, t)$$

$$w = w(r, z, t) \tag{1}$$

which is different from the conventional axisymmetric finite element in the appearing of v, the displacement in the circumferential direction. From this, the axisymmetric circumferentially vibrating modes can be obtained and will be shown later to be uncoupled from the motion of u and w. Displacements u and w are in the radial and the axial directions with r and z denoting the coordinates in those respective directions. t is the time variable. Since we are concerned with the axisymmetric vibration, all the three displacements are independent of the circumferential coordinate θ.

Strains can be derived from the displacements as follows:

$$\varepsilon_r = \frac{\partial u}{\partial r} \quad \varepsilon_z = \frac{\partial w}{\partial z} \quad \varepsilon_\theta = \frac{u}{r} \quad \gamma_{r\theta} = \frac{\partial v}{\partial r} - \frac{v}{r}$$

$$\gamma_{z\theta} = \frac{\partial v}{\partial z} \quad \gamma_{rz} = \frac{\partial u}{\partial z} + \frac{\partial w}{\partial r} \tag{2}$$

and the stress–strain relations are those for isotropic material,

$$\begin{Bmatrix} \sigma_r \\ \sigma_z \\ \sigma_\theta \\ \tau_{z\theta} \\ \tau_{r\theta} \\ \tau_{rz} \end{Bmatrix} = \begin{bmatrix} C_{11} & C_{12} & C_{13} & 0 & 0 & 0 \\ & C_{22} & C_{23} & 0 & 0 & 0 \\ & & C_{33} & 0 & 0 & 0 \\ & & & C_{44} & 0 & 0 \\ & \text{symmetry} & & & C_{55} & 0 \\ & & & & & C_{66} \end{bmatrix} \begin{Bmatrix} \varepsilon_r \\ \varepsilon_z \\ \varepsilon_\theta \\ \gamma_{z\theta} \\ \gamma_{r\theta} \\ \gamma_{rz} \end{Bmatrix} \tag{3}$$

with

$$C_{11} = C_{22} = C_{33} = \frac{E(1-\nu)}{(1+\nu)(1-2\nu)}$$

$$C_{12} = C_{13} = C_{23} = \frac{E\nu}{(1+\nu)(1-2\nu)}$$

$$C_{44} = C_{55} = C_{66} = G$$

where E is Young's modulus, ν is Poisson's ratio and G is the shear modulus. The strain energy is

$$U = \frac{1}{2}\int_v [\sigma_r\varepsilon_r + \sigma_z\varepsilon_z + \sigma_\theta\varepsilon_\theta + \tau_{z\theta}\gamma_{z\theta} + \tau_{r\theta}\gamma_{r\theta} + \tau_{rz}\gamma_{rz}]\,\mathrm{d}v \tag{4}$$

and the kinetic energy of the plate is written as

$$T = \frac{1}{2}\int_v \rho\Big[(\dot{u} - \Omega v)^2 + ((r+u)\Omega + \dot{v})^2 + \dot{w}^2\Big]\,\mathrm{d}v \tag{5}$$

where all the velocity components are measured with respect to an inertial frame, see Sreenivasamurthy and Ramamurti (1981), and Ω (rad/s) is the angular velocity of the plates. In conventional analyses, only the third term in the bracket is considered.

Following the general procedure of the finite element method, we express the displacements as

$$u = \sum_{i=1}^{n} u_i(t)N_i(r, z)$$

$$v = \sum_{i=1}^{n} v_i(t)N_i(r, z)$$

$$w = \sum_{i=1}^{n} w_i(t)N_i(r, z) \tag{6}$$

Where u_i, v_i, w_i are nodal values and N_i are shape functions, and n denotes the number of nodes in an element. We then substitute Eq. (6) into Eqs. (2)–(5) to express the strain energy and kinetic energy in terms of the nodal displacements and shape functions. After that, Hamilton's principle is applied to an element

$$\delta\left(\int_t (T - U)\,\mathrm{d}t\right) = 0 \tag{7}$$

and we end up with the following matrix equation

$$\begin{bmatrix} [m^{11}] & [m^{12}] & [m^{13}] \\ [m^{21}] & [m^{22}] & [m^{23}] \\ [m^{31}] & [m^{32}] & [m^{33}] \end{bmatrix} \begin{Bmatrix} \{\ddot{u}_j\} \\ \{\ddot{v}_j\} \\ \{\ddot{w}_j\} \end{Bmatrix} + \begin{bmatrix} [c^{11}] & [c^{12}] & [c^{13}] \\ [c^{21}] & [c^{22}] & [c^{23}] \\ [c^{31}] & [c^{32}] & [c^{33}] \end{bmatrix} \begin{Bmatrix} \{\dot{u}_j\} \\ \{\dot{v}_j\} \\ \{\dot{w}_j\} \end{Bmatrix} + \begin{bmatrix} [k^{11}] & [k^{12}] & [k^{13}] \\ [k^{21}] & [k^{22}] & [k^{23}] \\ [k^{31}] & [k^{32}] & [k^{33}] \end{bmatrix} \begin{Bmatrix} \{u_j\} \\ \{v_j\} \\ \{w_j\} \end{Bmatrix} = \begin{Bmatrix} \{f_i^r\} \\ \{f_i^\theta\} \\ \{f_i^z\} \end{Bmatrix} \tag{8}$$

In Eq. (8), $[[m_{ij}^{pq}]]$, $[[c_{ij}^{pq}]]$, $[[k_{ij}^{pq}]]$, for $i, j = 1 \sim n$, are the elemental mass, gyroscopic and stiffness matrices, respectively. $\{u_j\}$, $\{v_j\}$, $\{w_j\}$, $j = 1 \sim n$, are vectors of nodal displacements and $\{f_i^r\}$, $\{f_i^\theta\}$, $\{f_i^z\}$, $i = 1, \ldots, n$, are forcing vectors. For details of these matrices and vectors, see Appendix A. However, it is noteworthy that, from the expression of $\{f_i^r\}$, we may find that it is the centrifugal force of the rotating disk and our formulation automatically makes this term appear.

Eq. (8) for all the elements can be assembled to obtain the system equation for the annular plate.

$$[M]\{\ddot{U}\} + [C]\{\dot{U}\} + [K]\{U\} = \{F\} \tag{9}$$

Now we can turn to the first step of our approach: to calculate the internal stresses due to rotation by solving the simultaneous equations (10) below, which is obtained from Eq. (9) by dropping the time-dependent terms.

$$[K]\{U\} = \{F\} \tag{10}$$

After the rotation-induced stresses $\{\sigma^*\}$ are calculated from the solution of Eq. (10), integration of their multiplication with the nonlinear strains represents the part of contribution these stresses can make to the strain energy to affect the vibration of rotating annular plates.

$$V = \int_v \{\sigma^*\}^{\mathrm{T}} \times \{e_N\} \, \mathrm{d}v \tag{11}$$

where $\{\sigma^*\}^{\mathrm{T}} = [\sigma_r^* \ \sigma_z^* \ \sigma_\theta^* \ \tau_{rz}^*]$ and the nonlinear strains are

$$\{e_N\} = \begin{Bmatrix} \frac{1}{2}\left(\frac{\partial u}{\partial r}\right)^2 + \frac{1}{2}\left(\frac{\partial v}{\partial r}\right)^2 + \frac{1}{2}\left(\frac{\partial w}{\partial r}\right)^2 \\ \frac{1}{2}\left(\frac{\partial u}{\partial z}\right)^2 + \frac{1}{2}\left(\frac{\partial v}{\partial z}\right)^2 + \frac{1}{2}\left(\frac{\partial w}{\partial z}\right)^2 \\ \frac{1}{2}\left(\frac{u}{r}\right)^2 + \frac{1}{2}\left(\frac{v}{r}\right)^2 \\ \frac{\partial u}{\partial r}\frac{\partial u}{\partial z} + \frac{\partial v}{\partial r}\frac{\partial v}{\partial z} + \frac{\partial w}{\partial r}\frac{\partial w}{\partial z} \end{Bmatrix} \tag{12}$$

It should be noted that $\tau_{z\theta}^*$ and $\tau_{r\theta}^*$ are zero due to symmetry and the corresponding nonlinear strains are not shown in Eq. (12). The modified Hamiton's Principle then states:

$$\delta \int_t (T - U - V) \, \mathrm{d}t = 0$$

and we derive the modified elemental equation with the stiffness matrix being augmented as

$$\begin{bmatrix} [k^{11}] & [k^{12}] & [k^{13}] \\ [k^{21}] & [k^{22}] & [k^{23}] \\ [k^{31}] & [k^{32}] & [k^{33}] \end{bmatrix} + \begin{bmatrix} [g^{11}] & [g^{12}] & [g^{13}] \\ [g^{21}] & [g^{22}] & [g^{23}] \\ [g^{31}] & [g^{32}] & [g^{33}] \end{bmatrix} \tag{13}$$

and the remaining terms in Eq. (8) remain the same. The additional matrix $[[g^{pq}]]$ comes from Eq. (11) and are usually called the geometric stiffness matrix in the literature. Its detailed formulae can be found also in Appendix A.

Now we have the system equation in the following form.

$$[M]\{\ddot{U}\} + [C]\{\dot{U}\} + [[K] + [G]]\{U\} = \{F\} \tag{14}$$

To investigate the free vibration of spinning annular plates, synchronous harmonic motion is assumed and the gyroscopic matrix and the forcing term are neglected as is usually done (Leissa and Co, 1984), and we obtain the system eigenvalue equation as follows

$$[[K] + [G]]\{U\} = \omega^2[M]\{U\} \tag{15}$$

with ω^2 as the eigenvalue and ω is the natural frequency of axisymmetric vibration of the rotating annular plate. Also, a careful examination of the entries in the matrices of Eq. (15) shows that the motions in the radial and the thickness directions are uncoupled from those in the circumferential direction, and can be solved separately.

3. Results and discussions

To show the validation and accuracy of the present approach, some example problems with different ratios of inner-to-outer radius, ratios of radius-to-thickness, rotational speeds and boundary conditions are analyzed to calculate their natural frequencies. The material of the plate is steel with $E = 210$ GPa, $\nu = 0.3$ and $\rho = 7810$ kg/m^3. The geometry of the annular plate is of $a/h = 5$, 10, 20, 50 and $b/a = 0.1$, 0.25, 0.5 where h is the plate thickness and is assumed to be a constant throughout the investigation; a is the outer radius and b is the inner radius of the annular plate.

Three types of boundary conditions are employed in the present study: clamped-free (C-F), simply supported 1-free (SS1-F), and simply supported 3-free (SS3-F), see Fig. 1. These represent the most typical and practical boundary conditions of rotating disk in real situations. The two different simply supported boundary conditions have been studied by Liu and Chen (1995) and the abbreviations, SS1 and SS3, are thus followed. It is noted that SS3 is a condition that cannot be imposed with plate-theory-based approaches.

All the analyses are accomplished with a eight-node, two-dimensional quadratic isoparametric quadrilateral axisymmetric element, see Reddy (1993). Typical trends of convergence and meshes used in the present study are shown in Table 1. The numbers in the parentheses represent the numbers of grids of the finite element meshes in the radial and the thickness directions, respectively. Both are equally spaced. The finest mesh of each case in Table 1 is then employed to obtain frequencies in Tables 2 and 3. The rotational speed of the plate Ω and the natural frequency ω are nondimensionalized according to $\bar{\Omega} = \Omega a^2(\rho h/8D)^{1/2}$ and $\bar{\omega} = \omega a^2(\rho h/D)^{1/2}$, which are just the same as those in Sinha (1987) using a plate-theory-based approach with Mindlin's transverse shear deformation and rotary inertia terms considered.

Table 2 shows the nondimensional natural frequencies $\bar{\omega}_1$'s of the first axisymmetric transverse vibration mode of rotating annular plates under different combinations of a/h, b/a, boundary conditions

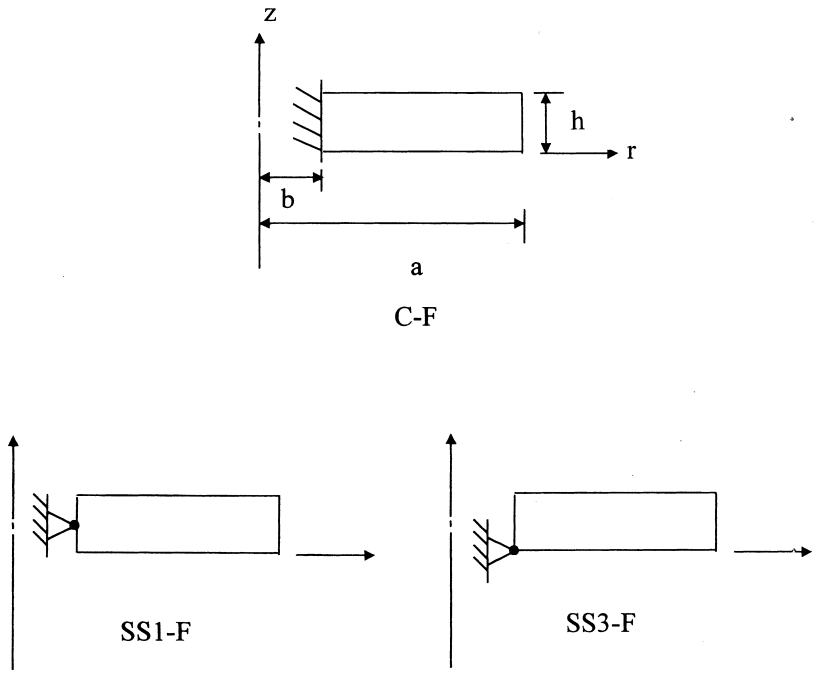

Fig. 1. Boundary conditions.

and $\bar{\Omega}$. The '$*$' symbol after a nondimensional frequency mean that there exists a circumferentially vibrating mode (in-plane torsional mode) before the present one. The shape of one such mode is shown in Fig. 2. From Table 2, the following conclusions may be drawn.

1. It is seen that $\bar{\omega}_1$'s get smaller with decreasing a/h for all the nonrotational cases with both the present method and Sinha's. As $\bar{\Omega}$ gets larger, the increase of $\bar{\omega}_1$ with decreasing a/h is more obvious for the present method than for Sinha for all the cases compared. With plate theories, centrifugal force due to rotation can cause only extension in the radial and the circumferential directions no matter what a/h is, when the initial stiffening is concerned. However, some other effect, such as Poisson's effect in r–z plane in the present 3D analysis, may make the rotating plate stiffer when the thickness is larger. In other words, the thickness effect for plate rotation is more significant in 3D analysis than in plate-theory analysis of plate vibrations. This might also be the reason that $\bar{\omega}_1$'s of Sinha's for smaller a/h are still smaller than for large a/h even when $\bar{\Omega}$ is eight and above and, the

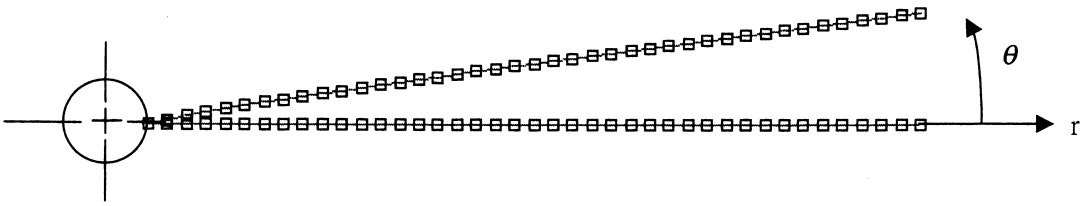

Fig. 2. An axisymmetric circumferentially vibrating mode (in-plane torsional mode), $\bar{\omega} = 6.568$, for C-F boundary condition, $b/a = 0.1$, $a/h = 10$, and $\bar{\Omega} = 4$ ($u = w = 0.0$).

boundary condition is of the clamped-free type.

2. Compared to the clamped-free cases, $\bar{\omega}_1$'s for the simply-supported boundary condition by Sinha are quite close to each other for various values of a/h, especially when $\bar{\Omega} = 0$. This could be attributed to the zero rotational boundary constraint that reduces the effect of thickness variation. Thus, $\bar{\omega}_1$ by Sinha for small a/h easily goes beyond that for larger a/h with increasing $\bar{\Omega}$, even though the thickness effect of the rotating plate in Sinha's analysis is not as high as in the 3D analysis.
3. For thin plates ($a/h = 50$), results of the present approach and those of Sinha's are very close when boundary conditions are C-F and SS1-F with arbitrary b/a and $\bar{\Omega}$. In these thin plate cases, Sinha switches his shear deformation theory to classical plate theory. Therefore, it is justified again that classical plate theory is a good alternative in analyzing the behaviors of thin plates in some cases, e.g., when the boundary conditions are the conventional C-F and SS1-F types.
4. In all cases, $\bar{\omega}_1$'s increase as $\bar{\Omega}$ increases. However, when $\bar{\Omega}$ is getting larger, the results for the C-F boundary condition and the SS1-F boundary condition become close to each other. For example, ratio of $\bar{\omega}_1$'s between C-F and SS1-F is 13.03/4.12 for $b/a = 0.5$, $a/h = 50$ at $\bar{\Omega} = 0$ and is 67.03/63.57 at $\bar{\Omega} = 16$. Therefore, we may say that the centrifugal effect dominates the vibration of the rotating disk at higher $\bar{\Omega}$ and makes the difference between the C-F and the SS1-F boundary conditions

Table 1
Typical convergence of $\bar{\omega}_1$ with meshes used in the present study ($\bar{\Omega} = 4$)

Mode 1

	$b/a = 0.1$				$b/a = 0.25$				$b/a = 0.5$			
Boundary conditions	a/h	5		10		5		10		5		10
C-F	(10 × 2)	9.637*	(10 × 2)	9.771*	(10 × 2)	12.74*	(10 × 2)	12.81	(10 × 2)	20.29	(10 × 2)	20.98
	(20 × 2)	9.623*	(20 × 2)	9.748*	(20 × 2)	12.73*	(20 × 2)	12.79	(10 × 4)	20.26	(20 × 2)	20.95
	(20 × 4)	9.611*	(20 × 4)	9.738*	(20 × 4)	12.71*	(20 × 4)	12.78	(20 × 4)	20.25	(20 × 4)	20.93
SS1-F	(10 × 2)	8.389*	(10 × 2)	8.561*	(10 × 2)	10.78*	(10 × 2)	10.82	(10 × 2)	15.76	(10 × 2)	16.02
	(20 × 2)	8.310*	(20 × 2)	8.516*	(20 × 2)	10.71*	(20 × 2)	10.76	(10 × 4)	15.64	(20 × 2)	15.97
	(20 × 4)	8.277*	(20 × 4)	8.476*	(20 × 4)	10.59*	(20 × 4)	10.69	(20 × 4)	15.56	(20 × 4)	15.87
SS3-F	(10 × 2)	7.779*	(10 × 2)	8.806*	(10 × 2)	9.891*	(10 × 2)	10.30	(10 × 2)	13.11	(10 × 2)	13.33
	(20 × 2)	7.594*	(20 × 2)	8.729*	(20 × 2)	9.779*	(20 × 2)	10.24	(10 × 4)	13.02	(20 × 2)	13.29
	(20 × 4)	7.434*	(20 × 4)	8.664*	(20 × 4)	9.656*	(20 × 4)	10.18	(20 × 4)	12.95	(20 × 4)	13.22

Mode 1

	$b/a = 0.1$				$b/a = 0.25$				$b/a = 0.5$			
Boundary conditions	a/h	20		50		20		50		20		50
C-F	(15 × 1)	9.874	(30 × 1)	9.873	(15 × 1)	12.88	(25 × 1)	12.88	(20 × 1)	21.24	(20 × 1)	21.31
	(15 × 2)	9.847	(60 × 1)	9.858	(15 × 2)	12.86	(50 × 1)	12.86	(20 × 2)	21.20	(40 × 1)	21.27
	(30 × 2)	9.830			(30 × 2)	12.84	(50 × 2)	12.85			(40 × 2)	21.26
SS1-F	(15 × 1)	8.764	(30 × 1)	8.777	(15 × 1)	11.11	(25 × 1)	11.13	(20 × 1)	16.38	(20 × 1)	16.45
	(15 × 2)	8.654	(60 × 1)	8.765	(15 × 2)	10.95	(50 × 1)	11.12	(20 × 2)	16.22	(40 × 1)	16.43
	(30 × 2)	8.624			(30 × 2)	10.92	(50 × 2)	11.05			(40 × 2)	16.37
SS3-F	(15 × 1)	9.009*	(30 × 1)	9.043	(15 × 1)	10.41	(25 × 1)	10.44	(20 × 1)	13.47	(20 × 1)	13.53
	(15 × 2)	8.965*	(60 × 1)	9.023	(15 × 2)	10.37	(50 × 1)	10.42	(20 × 2)	13.41	(40 × 1)	13.51
	(30 × 2)	8.921*			(30 × 2)	10.32	(50 × 2)	10.39			(40 × 2)	13.49

Table 2
Nondimensionalized frequencies of the first axisymmetric transverse vibration mode, $\bar{\omega}_1'$s, of rotating annular plates

		$b/a = 0.1$				$b/a = 0.25$				$b/a = 0.5$				
		a/h				a/h				a/h				
$\bar{\Omega}$	Boundary conditions	5	10	20	50	5	10	20	50	5	10	20	50	
	C-F	3.950*	4.167	4.225	4.241	5.455	5.747	5.825	5.842	11.61	12.65	12.97	13.03	Present
						5.56	5.76		5.83	11.97	12.71		13.02	Sinha (1987)
0	SS1-F	3.208*	3.392	3.436	3.448	3.232	3.329	3.352	3.359	3.985	4.088	4.113	4.120	Present
						3.33	3.35		3.37	4.09	4.15		4.16	Sinha (1987)
	SS3-F	3.505*	3.788*	3.899	3.969	4.135*	4.431	4.616	4.712	6.211	6.720	7.045	7.167	Present
	C-F	5.906*	6.163*	6.241	6.262	7.865	8.140	8.221	8.238	14.22	15.16	15.46	15.52	Present
						7.87	8.11		8.21	14.47	15.17		15.51	Sinha (1987)
2	SS1-F	4.963*	5.231	5.323	5.381	5.833	6.048	6.179	6.246	8.301	8.655	8.856	8.932	Present
						6.32	6.29		6.30	9.13	9.02		8.99	Sinha (1987)
	SS3-F	5.031*	5.593*	5.737	5.818	6.088*	6.477	6.608	6.692	8.304	8.801	9.076	9.181	Present
	C-F	9.611*	9.738*	9.830	9.858	12.71*	12.78	12.84	12.85	20.25	20.93	21.20	21.26	Present
						12.33	12.65		12.81	20.21	20.83		21.23	Sinha (1987)
4	SS1-F	8.277*	8.476*	8.624	8.765	10.59*	10.69	10.92	11.05	15.56	15.87	16.22	16.37	Present
						11.24	11.16		11.14	16.81	16.55		16.47	Sinha (1987)
	SS3-F	7.434*	8.664*	8.921*	9.023	9.656*	10.18	10.32	10.39	12.95	13.22	13.41	13.49	Present
	C-F		17.87*	17.56*	17.52		23.65*	23.22	23.14		35.77	35.74	35.74	Present
						22.46	22.79		23.07	34.79	35.10		35.70	Sinha (1987)
8	SS1-F		16.03*	15.90*	16.15		21.32*	21.19	21.32		31.68	31.76	31.93	Present
						21.70	21.53		21.49	32.91	32.29		32.11	Sinha (1987)
	SS3-F		15.11*	15.59*	15.67		18.69*	18.49	18.43		24.40	23.84	23.75	Present
	C-F		27.67*	25.66*	25.30		36.41*	34.17	33.70		52.69	51.48	51.24	Present
						33.01	33.27		33.64	50.61	50.45		51.19	Sinha (1987)
12	SS1-F		25.32*	23.70*	23.79		34.03*	31.99	31.81		49.41	47.78	47.69	Present
						32.33	32.08		32.00	49.21	48.21		47.91	Sinha (1987)
	SS3-F		22.35*	22.44*	22.33		29.00*	27.09	26.64		39.79	35.16	34.51	Present
	C-F		40.96*	34.28*	33.16*		52.59*	45.71*	44.39		71.85*	67.84	67.03	Present
						43.70	43.89		44.34	66.82	66.16		66.98	Sinha (1987)
16	SS1-F		38.16*	32.08*	31.59*		50.98*	43.42*	42.44			64.32	63.57	Present
						42.99	42.67		42.57	65.57	64.17		63.76	Sinha (1987)
	SS3-F		31.15	29.64*	29.03*		43.43	36.32*	34.96			47.46	45.48	Present

Table 3
Nondimensionalized frequencies of the second axisymmetric transverse vibration mode, $\bar{\omega}_2'$s, of rotating annular plates

		$b/a = 0.1$				$b/a = 0.25$				$b/a = 0.5$				
		a/h				a/h				a/h				
$\bar{\Omega}$	Boundary conditions	5	10	20	50	5	10	20	50	5	10	20	50	
	C-F	19.34	23.30*	24.77*	25.23	26.98*	33.49*	36.04*	36.87	50.33*	70.41*	80.77*	84.56	Present
						26.03	34.32		38.31	46.65	70.45		83.35	Sinha (1987)
0	SS1-F	16.67	19.68*	20.58*	20.84	22.44*	26.25*	27.40	27.74	41.96#	54.74*	59.34	60.76	Present
						23.30	27.86		29.79	44.88	56.10		61.87	Sinha (1987)
	SS3-F	16.05	21.22	22.76*	23.37	21.26*	28.40*	30.50*	31.27	38.76#	50.60*	61.32	64.22	Present
	C-F	23.21	26.74	28.11*	28.54	30.98*	36.93*	39.32*	40.11	54.18*	73.44*	83.51*	87.22	Present
						28.72	37.89		42.51	47.84	72.47		88.55	Sinha (1987)
2	SS1-F	20.62	23.36	24.25*	24.58	26.74*	30.27*	31.49*	31.94	47.06#	58.61*	63.10	64.55	Present
						27.42	31.60		33.41	51.09	60.16		64.37	Sinha (1987)
	SS3-F	19.44	24.47	25.98*	26.54*	24.38	31.27*	33.34*	34.07	40.89#	52.32*	63.18	66.10	Present
	C-F	32.79	35.23	36.35*	36.72*	41.13+	45.80*	47.84*	48.52	64.38#	81.90*	91.24*	94.72	Present
						36.38	46.87		52.35	53.84	79.23		96.86	Sinha (1987)
4	SS1-F	30.16	32.13	32.94*	33.38*	37.22+	40.03*	41.31*	41.97	58.82#	68.84*	73.14	74.68	Present
						36.51	41.45		43.60	60.59	69.92		74.19	Sinha (1987)
	SS3-F	27.87	32.41	33.89	34.37*	35.57+	38.73*	40.73*	41.39	47.72#	57.04*	68.46*	71.43	Present
	C-F		59.19	58.82	58.86*		72.06	72.53*	72.80		109.7*	117.1*	119.8	Present
						57.86	72.37		80.06	75.17	103.17		123.64	Sinha (1987)
8	SS1-F		56.11	55.69	56.08*		67.20	67.45*	67.91		99.96*	103.5*	104.9	Present
						59.89	67.44		70.71	88.19	99.16		104.44	Sinha (1987)
	SS3-F		54.41	55.22	55.40*		60.62	62.30*	62.55		94.27#	86.70*	89.67	Present
	C-F		89.83+	84.41	83.41*		105.7+	101.5*	100.8*		146.4#	150.6*	152.6	Present
						81.92	101.49		111.84	101.01	134.05		158.23	Sinha (1987)
12	SS1-F		86.52+	81.23	80.80*		101.6+	96.91*	96.51*		140.0#	139.7*	140.7	Present
						85.34	95.92		100.49	121.90	133.73		140.27	Sinha (1987)
	SS3-F		82.64+	79.32	78.60*		94.47+	87.80*	87.03*		125.7#	111.3*	113.9	Present
	C-F		131.3+	112.2	108.8		149.1+	133.1	130.1*		190.0+	188.1*	188.7	Present
						106.82	131.83		145.04	128.45	167.93		196.59	Sinha (1987)
16	SS1-F		128.1#	108.8	106.3		147.8+	128.7	126.1*		188.6#	178.9*	178.5	Present
						111.51	125.25		131.17	159.49	170.25		178.22	Sinha (1987)
	SS3-F		119.8#	105.4	102.6		141.4+	115.7	112.8*			139.5*	141.2	Present

insignificant.

5. The nondimensional fundamental frequencies $\bar{\omega}_1$'s of a rotating disk with SS3-F, a type of boundary condition which is not possible to be represented by plate-theory-based approaches, are quite different from those of SS1-F. When $\bar{\Omega}$ is smaller, $\bar{\omega}_1$'s of SS3-F are higher than those of SS1-F and lower than those of C-F, but they become the lowest among the three boundary conditions when $\bar{\Omega}$ becomes larger. This may attribute to the unsymmetric constraint of the SS3-F and the induced nonuniform stiffening across the thickness due to rotation, i.e., with one half part of the thickness being stiffer than the other half might make the flexural rigidity of the plate lower than a uniformly stiffened one.
6. The nondimensional fundamental frequencies $\bar{\omega}_1$'s increase with the increase of b/a for all cases. However, smaller b/a makes smaller difference in $\bar{\omega}_1$ for different boundary conditions than would large b/a at $\bar{\Omega} = 0$, 2 or 4. This is reasonable because, when b/a becomes smaller or the annular plate is approaching a whole plate, inside boundary conditions will make little difference. However for large $\bar{\Omega}$, the centrifugal effect, instead of b/a, will dominate as stated in 4 and 5.

Some typical results are shown graphically in Figs. 3 and 4 which compare the trends of $\bar{\omega}_1$ between the present approach and Sinha (1987). The centrifugal effect is shown in Fig. 5. Differences of C-F, SS1-F and SS3-F are shown in Figs. 6 and 7 demonstrates the significance of change of b/a.

It is also noteworthy that, during the investigation, some circumferentially vibrating modes were revealed. These modes have not been seen in the conventional analyses of rotating plates, at least to the authors' knowledge. From the results shown, it seems that higher $\bar{\Omega}$ and/or lower b/a and a/h may trigger the circumferential vibrating modes, and surprisingly, they are the lowest modes in some cases.

The frequencies $\bar{\omega}_2$ of the second axisymmetric transverse vibrating mode are also shown in Table 3 together with some results appearing in Sinha (1987). In Table 3, the '$*$' means the same thing as in

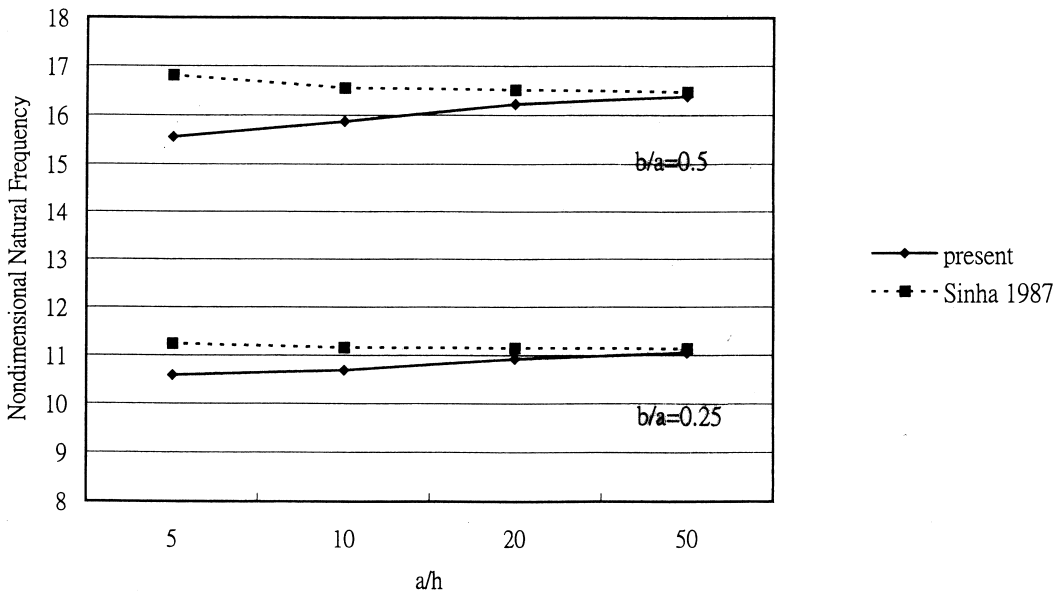

Fig. 3. Comparsion of the trend of $\bar{\omega}_1$ with changing a/h between the present method and that of Sinha (1987) for $\bar{\Omega} = 4$ and simply supported boundary condition.

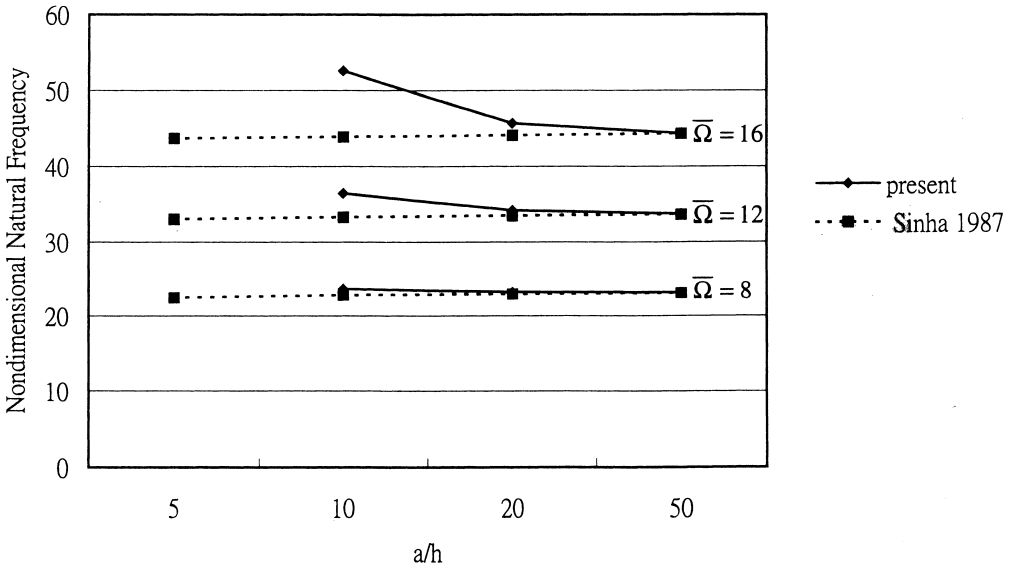

Fig. 4. Comparsion of the trend of $\bar{\omega}_1$ with changing a/h between the present method and that of Sinha (1987) for C-F and $b/a = 0.25$.

Table 2, while the '+' and '#' symbols after a nondimensional frequency denote that there exists a straining mode (Liu and Lee, 1997) or both a straining mode and a circumferentially vibrating mode before the present one. The stiffening effect of $\bar{\omega}_2$ due to the variations of thickness and rotational speed is of the same, though weaker, trend as $\bar{\omega}_1$, so the explanation we made for $\bar{\omega}_1$ can be applied as well to

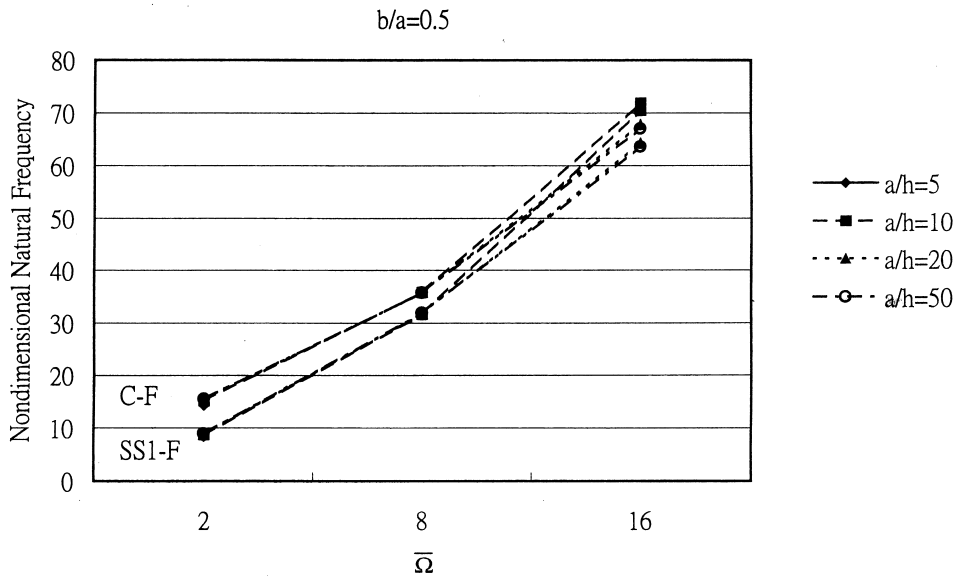

Fig. 5. Typical effect of centrifugal force on $\bar{\omega}_1$.

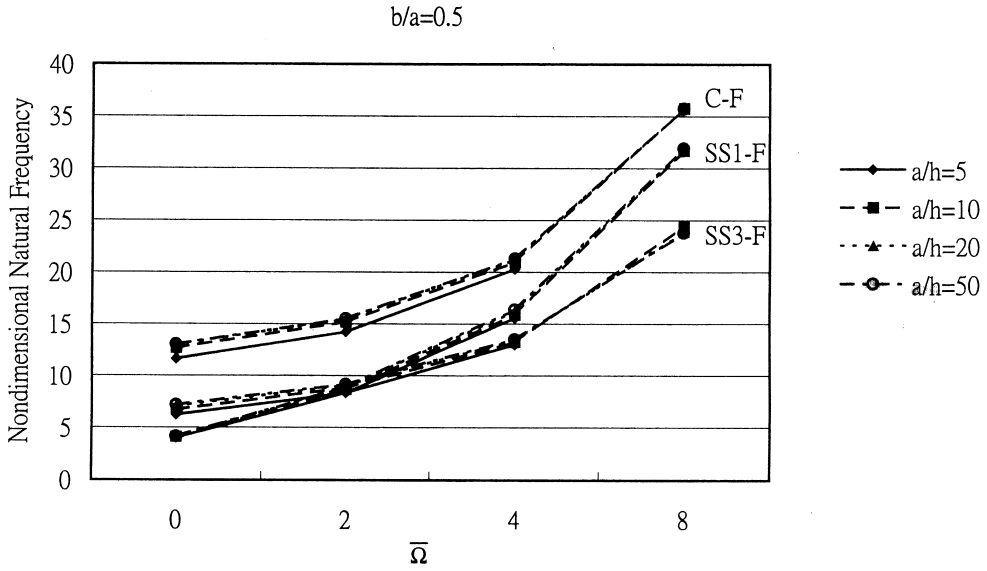

Fig. 6. Typical effect of boundary conditions on $\bar{\omega}_1$ with changing $\bar{\Omega}$ and $b/a = 0.5$.

$\bar{\omega}_2$. However, it is interesting to note that better matching of $\bar{\omega}_2$ between C-F and SS1-F exists for most of the cases. This is true for both the 3D and 2D analyses. Since $\bar{\omega}_1$ and $\bar{\omega}_2$ have the same trend, the better matching of the second frequencies could be attributed to the weaker effect of boundary difference on $\bar{\omega}_2$ than on $\bar{\omega}_1$.

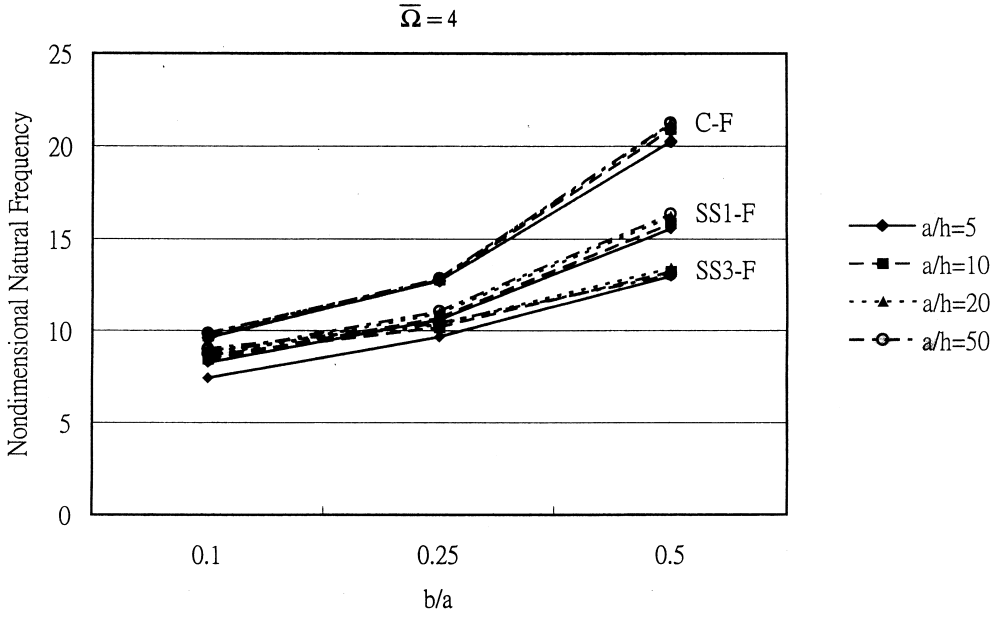

Fig. 7. Typical effect of b/a on $\bar{\omega}_1$.

Table 4
Comparisons of the first ten vibration frequencies in $\omega a\sqrt{\rho/G}$ for a circular plate and two annular plates by the present method (all with 10×4 mesh) and by the 3D Ritz method (Tables 8, 9, 14, and 15 in So and Leissa, 1998) with $\nu = 0.3$[a]

Circular plate $a/h = 2.5$		Annular plate $a/h = 2.5$			
		$b/a = 0.1$		$b/a = 0.5$	
Present	So and Leissa	Present	So and Leissa	Present	So and Leissa
1.464	1.464 ($1A0^a$)	1.433	1.433 ($1A0^a$)	1.388	1.388 ($1A0^a$)
3.436	3.436 ($1S0^a$)	3.319	3.319 ($1S0^a$)	2.233	2.234 ($1S0^a$)
4.417	4.415 ($2A0^a$)	4.493	4.491 ($2A0^a$)	6.814	6.814 ($1S0^t$)
5.136	5.136 ($1S0^t$)	5.142	5.142 ($1S0^t$)	7.856	7.854 ($1A0^t$)
7.360	7.353 ($3A0^a$)	7.439	7.432 ($3A0^a$)	8.324	8.321 ($2A0^a$)
7.856	7.854 ($1A0^t$)	7.856	7.854 ($1A0^t$)	9.133	9.127 ($3A0^a$)
8.419	8.417 ($2S0^t$)	8.163	8.161 ($2S0^a$)	9.958	9.957 ($2S0^a$)
8.589	8.589 ($2S0^a$)	8.459	8.457 ($2S0^t$)	10.40	10.398 ($2A0^t$)
9.335	9.323 ($4A0^a$)	9.389	9.388 ($2A0^t$)	11.37	11.343 ($3S0^a$)
9.386	9.384 ($2A0^t$)	9.632	9.620 ($4A0^a$)	12.22	12.207 ($4S0^a$)

[a] The number in the parentheses represents the mode number. 'A' means antisymmetric mode and 'S' symmetric mode (with respect to the midplane of the plate). 0^a represents axisymmetric mode and 0^t torsional mode. See So and Leissa (1998) for more details.

It should be mentioned here that due to the high rotating speeds of the plate with $a/h = 5$, the terms in the stiffness matrix that include Ω may make the stiffness matrix non-positive definite (Meirovitch, 1980). The frequencies for $a/h = 5$ at $\bar{\Omega} = 8$, 12 and 16 are thus not shown, so are those for $b/a = 0.5$ with SS1-F ($\bar{\omega}_1$ only) and SS3-F at $\bar{\Omega} = 16$. Also, it should be noted that the induced stresses of some cases in Tables 2 and 3 may already be higher than the ultimate strength of the material for higher rotational speeds of the plate.

To further justify the accuracy of the present method, natural frequencies of some typical circular and annular nonrotating plates with completely free boundary condition by the present method are also compared to those by an accurate 3D Ritz method (So and Leissa, 1998) in Table 4. The natural frequencies are found to agree very well between these two methods with corresponding modes having the same mode shapes. The validation of the present method can thus be reassured. Also, it should be emphasized that some of the vibration modes, shown in both the present results and those of So and Leissa (1998), are only possible with 3D analysis.

4. Conclusions

In the present study, a modified axisymmetric finite element, based on 3D elasticity, is employed in the axisymmetric vibration analyses of rotating annular plates. The approach can take into account the centrifugal effect by considering all of the four nonzero rotation-induced stresses instead of only two in the conventional analyses, can include in the kinetic energy all the velocity components in the three coordinate directions instead of only one as usually shown in the literature, and can impose on another type of simply supported condition which just cannot be done by plate-theory-based approaches. Moreover, it enables us to conduct a 3D analysis with a two-dimensional finite element.

Results of some example problems by the present method are shown in tables and figures, and are compared with those by a typical conventional approach. The most remarkable difference between the

present method and the conventional one is that thickness effect of rotating plates is usually more significant in the present 3D analysis than in Sinha's. This effect becomes more obvious for larger rotational speeds. Also, cases with SS3-F can be analyzed with the present method and the results are quite different from those with the conventional simply supported boundary condition. However, for thin plate, both the present and the conventional approaches will get very close results even for high rotational speeds.

For circumferentially vibrating modes, a more thorough study will be needed to know the conditions for their appearance, their interaction or relation with the transverse vibrating modes, etc. and their investigation will be conducted in another research project.

Appendix A

$$k_{ij}^{11} = \int_v \left[C_{11} N_{i,\,r} N_{j,\,r} + C_{13} \frac{1}{r} N_{i,\,r} N_j + C_{13} \frac{1}{r} N_i N_{j,\,r} + C_{33} \frac{1}{r^2} N_i N_j. + C_{66} N_{i,\,z} N_{jz} - \rho \Omega^2 N_i N_j \right] \mathrm{d}v$$

$$k_{ij}^{13} = k_{ji}^{31} = \int_v \left[C_{12} N_{i,\,r} N_{j,\,z} + C_{23} \frac{1}{r} N_i N_{j,\,z} + C_{66} N_{i,\,z} N_{j,\,r} \right] \mathrm{d}v$$

$$k_{ij}^{22} = \int_v \left[C_{55} N_{i,\,r} N_{j,\,r} - C_{55} \frac{1}{r} \left(N_{i,\,r} N_j + N_i N_{j,\,r} \right) + C_{55} \frac{1}{r^2} N_i N_j + C_{44} N_{i,\,z} N_{j,\,z} - \rho \Omega^2 N_i N_j \right] \mathrm{d}v$$

$$k_{ij}^{33} = \int_v \left[C_{22} N_{i,\,z} N_{j,\,z} + C_{66} N_{i,\,r} N_{j,\,r} \right] \mathrm{d}v$$

$$k_{ij}^{12} = k_{ji}^{21} = k_{ij}^{23} = k_{ji}^{32} = 0$$

$$g_{ij}^{11} = \int_v \left[\sigma_r^* N_{i,\,r} N_{j,\,r} + \sigma_z^* N_{i,\,z} N_{j,\,z} + \sigma_\theta^* \frac{1}{r^2} N_i N_j + \tau_{rz}^* \left(N_{i,\,z} N_{j,\,r} + N_{i,\,r} N_{j,\,z} \right) \right] \mathrm{d}v$$

$$g_{ij}^{22} = \int_v \left[\sigma_r^* N_{i,\,r} N_{j,\,r} + \sigma_z^* N_{i,\,z} N_{j,\,z} + \sigma_\theta^* \frac{1}{r^2} N_i N_j + \tau_{rz} \left(N_{i,\,z} N_{j,\,r} + N_{i,\,r} N_{j,\,z} \right) \right] \mathrm{d}v$$

$$g_{ij}^{33} = \int_v \left[\sigma_r^* N_{i,\,r} N_{j,\,r} + \sigma_z^* N_{i,\,z} N_{j,\,z} + \tau_{rz}^* \left(N_{i,\,z} N_{j,\,r} + N_{i,\,r} N_{j,\,z} \right) \right] \mathrm{d}v$$

$$g_{ij}^{12} = g_{ji}^{21} = g_{ij}^{13} = g_{ji}^{31} = g_{ij}^{23} = g_{ji}^{32} = 0$$

$$c_{ij}^{11} = c_{ij}^{22} = c_{ij}^{23} = c_{ji}^{32} = c_{ij}^{33} = c_{ij}^{13} = c_{ji}^{31} = 0$$

$$c_{ij}^{12} = \int_v \left(-2\rho\Omega N_i N_j \right) \mathrm{d}v$$

$$c_{ji}^{21} = \int_v \left(2\rho\Omega N_i N_j \right) \mathrm{d}v$$

$$m_{ij}^{11} = m_{ij}^{22} = m_{ij}^{33} = \int_v \left(\rho N_i N_j \right) \mathrm{d}v$$

$$m_{ij}^{12} = m_{ji}^{21} = m_{ij}^{13} = m_{ji}^{31} = m_{ij}^{23} = m_{ji}^{32} = 0$$

$$f_i^r = \int_v \rho\Omega^2 r N_i \, \mathrm{d}v$$

$$f_i^\theta = f_i^z = 0$$

References

Barasch, S., Chen, Y., 1972. On the vibrations of a rotating disk. Trans. ASME, J. Appl. Mech. 39, 1143–1144.

Eversman, W., Dodson, R.O., 1969. Free vibration of a centrally clamped spinning circular disk. AIAA J. 7, 2010–2013.

Kirkhope, J., Wilson, G.J., 1976. Vibration and stress analysis of thin rotating discs using annular finite elements. J. Sound Vib. 44, 461–474.

Lee, H.P., Ng, T.Y., 1995. Vibration and critical speeds of a spinning annular disk of varying thickess. J. Sound Vib. 187, 39–50.

Leissa, A.W., 1977. Recent research in plate vibration, 1973–1976: complicating effects. Shock Vib. Dig. 9, 21–35.

Leissa, A.W., 1981. Plate vibration research, 1976–1980: complicating effects. Shock Vib. Dig. 13, 19–36.

Leissa, A.W., Co, C.M., 1984. Coriolis effects on the vibrations of rotating beams and plates. In: Proc. 12th Southeast. Conf. Theoret. Appl. Mech., 508–513.

Leissa, A.W., 1987. Recent studies in plate vibrations: 1981–1985 part II. complicating effects. Shock Vib. Dig. 19, 10–24.

So, J., Leissa, A.W., 1998. Three-dimensional vibrations of thick circular and annular plates. J. Sound Vib. 209 (1), 15–41.

Liu, C.F., Chen, G.T., 1995. A simple finite element analysis of axisymmetric vibration of annular and circular plates. Int. J. Mech. Sci. 8, 861–871.

Liu, C.F., Lee, Y.T., 1997. Axisymmetric straining modes in the vibration of circular plates. J. Sound Vib. 208 (1), 47–54.

Meirovitch, L., 1980. Computational Methods in Structural Dynamics. Sijthoff and Noordhoff, Alphen, p. 39.

Nigh, G.L., Olson, M.D., 1981. Finite element analysis of rotating disks. J. Sound Vib. 77 (1), 61–78.

Rajguru, A., Sundararajan, V., 1982. Vibration of a rotating orthotropic disk. Trans. ASME, J. Appl. Mech. 49, 654–656.

Reddy, J.N., 1993. An Introduction to the Finite Element Method, 2nd ed. McGraw-Hill, New York, p. 417.

Sinha, S.K., 1987. Determination of natural frequencies of a thick spinning annular disk using a numerical Rayleigh–Ritz's trial function. J. Acoust. Soc. Am. 81, 357–369.

Sreenivasamurthy, S., Ramamurti, V., 1981. A parametric study of vibration of rotating pre-twisted and tapered low aspect ration cantilever plates. J. Sound Vib. 76 (3), 311–328.

Wilson, G.J., Kirkhope, J., 1976. Vibration analysis of axial flow turbine disks using finite element. ASME J. Eng. Ind. 1008–1013.